

Understanding a frequency shifting phenomenon interfering with in-line acoustic monitoring of an extrusion compounding process for polymer composites

Journal of Thermoplastic Composite Materials

2025, Vol. 0(0) 1–19

© The Author(s) 2025



Article reuse guidelines:

sagepub.com/journals-permissions

DOI: 10.1177/08927057251321492

journals.sagepub.com/home/jtc



Austin D Bedrosian¹ , Andrew Hrymak², Gisela Lanza³ and Michael R Thompson¹

Abstract

This study investigated an anomalous frequency shift observed in collected spectra from an inline monitoring system based on guided ultrasonic waves, with the changing flow rate of an extrusion compounding process for fiber-reinforced thermoplastics. Three possible process parameters to explain the ultrasonic peak shifting, namely melt temperature, velocity, and fiber length were evaluated. The unlikely potential of a doppler moment due to melt velocity, was readily dismissed in the analysis since fluid flow through the die was too slow and while resonance frequency variation may be possible from the related fiber damage associated with increasing flow rates, there was insufficient physical evidence of this anticipated effect in this study. Melt temperature variation associated with viscous dissipation was concluded to be the dominant cause for the frequency shifting noted in the acoustic spectra. The changes in material temperature through which the sound travelled were varying the extent and frequency of the dispersion modes in the polymer melt. These findings are new guidance to processors on setting up a system using active ultrasonics for in-line monitoring in the polymer composites industry.

¹Department of Chemical Engineering, CAPPA-D/MMRI, McMaster University, Hamilton, ON, Canada

²Department of Chemical and Biochemical Engineering, University of Western Ontario, London, ON, Canada

³Institute of Production Science (wbk), Karlsruhe Institute of Technology (KIT), Karlsruhe, Germany

Corresponding author:

Michael R Thompson, Department of Chemical Engineering, McMaster University, 1280 Main St W, Hamilton, ON L8S 4L7, Canada.

Email: mthomps@mcmaster.ca

Keywords

Guided ultrasonics, fiber-reinforced polymer composite, compounding, acoustic dispersion, in-line monitoring

Introduction

Polymer composite materials offer designers and engineers with a novel capability of mass producing complex, lightweight parts meant for structural application in place of metals. The ability to reinforced inexpensive and chemically inert polymer matrices with readily available short- or long-length fibers has increased demand for composite materials in the automotive, aerospace and energy sectors.¹ With their increased use in manufacturing, the anisotropic nature of these fibers within a polymer matrix add new challenges that need addressing like developing reliable quality assurance tools for these composite materials.

The use of sound waves to non-destructively quantify materials has been used for decades.² The ability to assess a material and obtain information related to its structural integrity, without the need to destroy it, is invaluable for parts intended to remain in service or too high in value to be used in quality assurance during production, for example. Ultrasonic waveforms are commonly considered for this non-destructive testing to minimize ambient interference, being used in a variety of engineering fields to characterize the integrity of materials, such as concrete or polymers, from their exposure to aggressive environments.^{3,4} One driving factor in implementing non-destructive acoustic monitoring techniques in manufacturing right now is the shift towards industrial digitization. This philosophy requires inline or online sensors used on either batch or continuous processes and often demand integrating very large data sets with computational models to monitor material properties in real-time and, when necessary, adjust the process before substantial off-spec product is generated as waste. There are a variety of technologies that can be utilized for monitoring, including ultrasonic transducers which are the focus of this paper.^{5–8} The benefits of using ultrasonic transducers for advanced manufacturing applications is their low capital cost relative to other methods, and ease of integration with current manufacturing systems.

With regards to the information obtained by ultrasonic sensors, the recorded sound waves can be expressed in either the time-domain, as an amplitude-time waveform or in the frequency-domain as an amplitude-frequency spectra. There is a great amount of literature on time-domain analysis, where artifacts within a material can be observed, localized density changes can be monitored, and the underlying composition of a material can be determined.^{9–12} The frequency domain is considered to contain a dense collection of unique data that has been previously disregarded in real-time acoustic monitoring due to the complexity of postprocessing the obtained signals. However, with less expensive computational power now available and the new ability to remotely access data in the cloud, the handling and storage issues with large datasets associated

with the frequency-domain are now more feasibly analyzed using computational non-linear models. Furthermore, passive and active testing is possible where acoustic emissions associated with the rapid release of energy within a material are detected in the passive case,¹³ or an acoustic sensor emits propagating waves of predetermined frequencies that are subsequently monitored in the active case.¹⁴ Distinctive information can be obtained about the material in question using an active method, such as predicting the fiber orientation in composite materials, observing crack propagation within materials, monitoring polymer flow, or quantifying the degree of polymerization during production.^{14–16}

For frequency domain bulk assessment of single- or multiple-material properties arising from a continuous process, a novel area of focus is the integrity of received signals during in-line monitoring. This concern arose while translating a newly developed active ultrasonic method from benchtop¹⁴ to a continuous extrusion system where the authors noticed frequency shifts of spectral peaks in the detected signals while studying process variables despite the highly unlikely case of doppler shifting. The purpose of this study was to first verify the observed frequency shifting was a physical attribute of the glass-fiber polypropylene compounding process rather than being an artifact of data collection/processing and then to understand the cause for the phenomenon. The goal of the study was to devise guidance on using in-line active ultrasonic monitoring for polymer composite processing applications.

Materials and methods

Materials

The chosen resin was an extrusion-grade HL781G isotactic polypropylene (LyondellBasell; Texas, USA) supplied in pellet form. Chopped glass fibers with sizing applied for polyolefin applications were supplied from Dow-Corning for reinforcement. The fibers had an average fiber length and diameter of 4 mm and 14 μ m, respectively (data provided by the supplier), and were dried at 80°C for 24 hours prior to use in order to eliminate moisture. Polybond 3200 maleated polypropylene compatibilizer (SI Group; New York, USA) was blended with the matrix resin at 1.5 wt% to improve cohesion between the polypropylene and fibers.

Composite preparation

An 18 mm 40 L/D co-rotating intermeshing twin screw extruder (Leistritz Extrusion Technology; New Jersey, USA) was used to compound the different composite formulations (0–40% fiber loading). The screws were designed to allow adequate wetting and mixing of the fibers into the polypropylene melt, as seen in the supplementary documentation, [Figure S1](#). Each composite formulation was fed into the extruder at varying mass flow rates ranging from 0.50 to 2.00 kg/h. The screw speed was set to 100 RPM. The temperature inside the extruder barrel of Zone 1 was maintained at 180°C with the other zone temperatures, Zones 2 to 6, set to 225, 230, 230, 245, 245 and 220°C respectively. The slit die with 40 mm (W) \times 2 mm (H) opening was used to prepare sample tapes, with its temperature set to 210°C. The extrudate was pulled from the extruder and

air cooled, resulting in a tape with an average width of 34.31 mm and thickness of 1.86 mm. Melt temperature of the polymer was monitored continuously using a FLIR E5 thermal camera (FLIR, Oregon, USA) positioned at the outlet of the die. The melt temperature measurement was intermittently validated with a thermocouple immersed into the extrudate melt.

Fiber length distribution

Solidified extruded tapes collected at 80 and 320 mm/min melt velocities (corresponding to mass flow rates of 0.5 kg/h and 2 kg/h) for polymer composites with 10 wt% or 40 wt% glass fiber content, were cut to 2.54 cm lengths for ashing. These fiber weight fractions and velocities were chosen to observe the fiber length distribution spanning the lowest and highest shear stress conditions of the trials. Ashing was conducted in a Sentry Xpress 4.0 furnace (Paragon, Texas, USA) preheated to 600°C, with samples in ceramic dishes placed within 1 hour to remove all organics. The collected fibers were spread out on a glass slide and imaged with a VistaVision optical microscope (VWR International, Pennsylvania, USA). Multiple cut lengths of a sample were evaluated by this approach until a minimum of 1000 fibers could be measured; fiber lengths in the images were measured using ImageJ software (National Institute of Health, USA). An example microscopic image used for measurement is shown in the supplementary documentation, [Figure S2](#). Repeated trials for two conditions were assessed for uncertainty: 10 wt%/80 mm/min and 40 wt%/320 mm/min. A probability density function (PDF) and a cumulative distribution function (CDF) were fit to the measured fibers to better articulate the distribution; the non-parametric (χ^2) PDF fit the fiber length data with the lowest standard error compared to parametric PDF (Gaussian, Tophat, Epanechnikov, Exponential, Linear, Cosine). Both the PDFs and CDFs can be seen in [Figure 1](#).

Acoustic setup

The monitoring method used active ultrasonics which was adapted from previous work for composite fiber orientation analysis.¹⁴ An emitter (resonant type, R15 α) and receiver (broadband type, F30 α) ultrasonic sensor (Physical Acoustic Corporation; New Jersey, USA) were fit into polyether ether ketone (PEEK) mounting rods using silicone vacuum grease (Dow Corning, Michigan, USA) as a coupling agent to limit signal loss. The choice of PEEK was to isolate the sensors from the high temperature of the extruder die while allowing adequate signal propagation into and from the polymer melt. The PEEK rods were screwed into the slit die, as seen in [Figure 2](#), allowing for transmission of the acoustic signal through the polymer melt passing within the die. Custom Command Expert script (Keysight, California, USA) was used to analyze 31 consecutive square waveforms, each comprised of 10 cycles at a fixed frequency, produced in the extruded melt using a 10 MHz Waveform generator (Agilent) connected to the emitting sensor. The frequency was stepped up in 1 kHz increments, from 220 kHz to 250 kHz; this frequency range was selected based on calculations assuming the glass fibers resonate like beams.¹⁴ The received signal for each waveform, after passing through the melt, was amplified with a

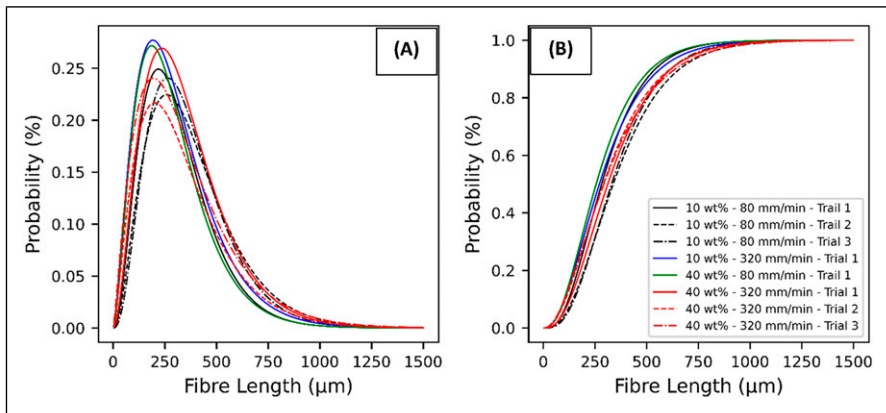


Figure 1. Representation of the fiber length distributions. (A) is the probability density function using a χ^2 distribution to fit the measured fibers. (B) is the cumulative distribution functions generated from the probability density functions to import the accuracy of the Kolmogorov-Smirnov tests.

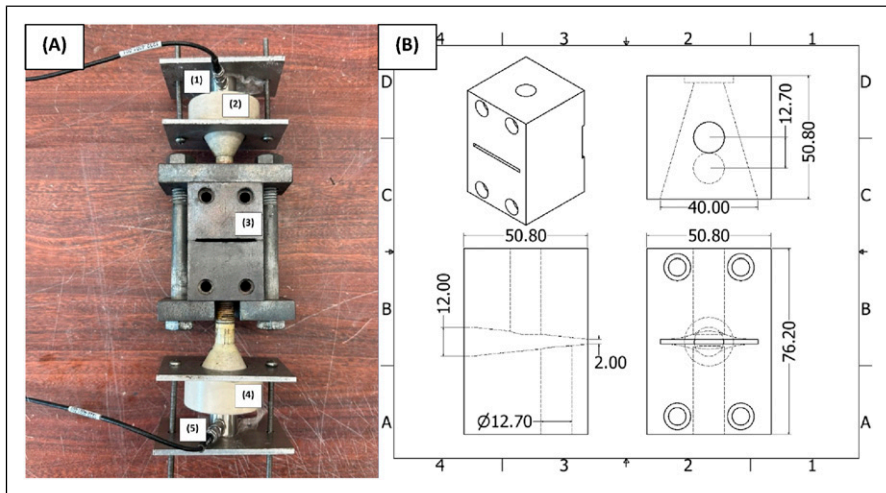


Figure 2. Custom acoustic die for 18-mm twin screw extruder. (A) is die setup with the acoustic system. The emitting sensor (1), coupled to a PEEK buffer rod (2) with silicon vacuum grease transmits the ultrasonic signals through the composite melt within the die (3) towards the second PEEK buffer rod (4) which transmits the signal to the receiving sensor (5). The die is a circle-to-slit die, with the polymer exiting as a rectangular tape. (B) is the Autodesk Inventor drawing for the die with the associated measurements. All values report are in mm.

60 dB gain and recorded with a 12-bit 4-channel 10 MHz data acquisition system (National Instruments, Texas, USA). The sampling rate was set to 3 MHz with a noise threshold of 0.03 Volts to limit baseline noise; the noise threshold was set to filter extraneous vibrations produced by the extruder. The recorded signals were converted into the frequency domain by Fast Fourier transformation (FFT) using custom made Python code (version 3.11) with libraries NumPy and SciPy. Instead of using the entire FFT spectrum, a frequency range of 200 to 320 kHz was used since this was the frequency range that yielded the greatest amount of information. This range was discretized subsequently into 1 kHz bands to yield 121 frequency bands. A minimum of 40 signals were randomly recorded at different times during an extrusion run, spanning various days.

Ultrasound signal analysis

The results of the statistical analysis discussed in the statistical methods section indicated clear differences in the spectrum exist for each weight fraction. The spectrum at each melt velocity was plotted to determine if any trends/ changes in the frequency domain could be identified. It appeared by this analysis that only distinctive peaks within the spectrum were consistently changing with increasing melt velocity and not by changes in fiber content. Some of those distinctive peaks were shifting towards higher frequencies while others were shifting towards lower frequencies, with increasing melt velocity. A Python script using the SciPy '*find peaks*' function was developed to seek the frequency bands varying uniquely in the extruded composite melt. The script identified the frequency and amplitude of local maxima (peaks) in the spectrum of collected signals from trials varying fiber content and melt velocity. This analysis was independent from the PCA analysis as the entire spectrum was analyzed to identify and select peaks. This peak selection is demonstrated in [Figure 3](#), where the identified peaks found by the script are marked with an 'x'. A distribution of the frequency values for the located peaks were made for each fiber content where the y-axis was the number of peaks identified and the x-axis being the spectrum frequency. This resulted in a multimodal distribution consistently appearing for each fiber content. These multimodal distributions were compared based on fiber content to identify which frequencies and frequency bands were consistently identified as a peak by the script. Instead of using the exact frequency for the peak, the surrounding regions (frequency bands) that were consistent in every fiber content were identified as distinctive peaks. Peaks only seen for one fiber content but not the others were not included for analysis. As a result, twelve peaks were identified as varying with melt velocity for all the different fiber contents examined, at 222–227 kHz, 227–229 kHz, 229–232 kHz, 232–235 kHz, 235–240 kHz, 240–244 kHz, 252–255 kHz, 258–261 kHz, 261–264 kHz, 264–266 kHz, 266–269 kHz and 269–272 kHz.

Dispersion mode determination

An important calculation for conducting acoustic monitoring is the calculation of dispersion modes. In all materials there exist frequencies where the propagated acoustic waves travel with limited resistance through the material medium. The mechanical waves force the material to expand/contract as they travel throughout the medium, being highly dependent

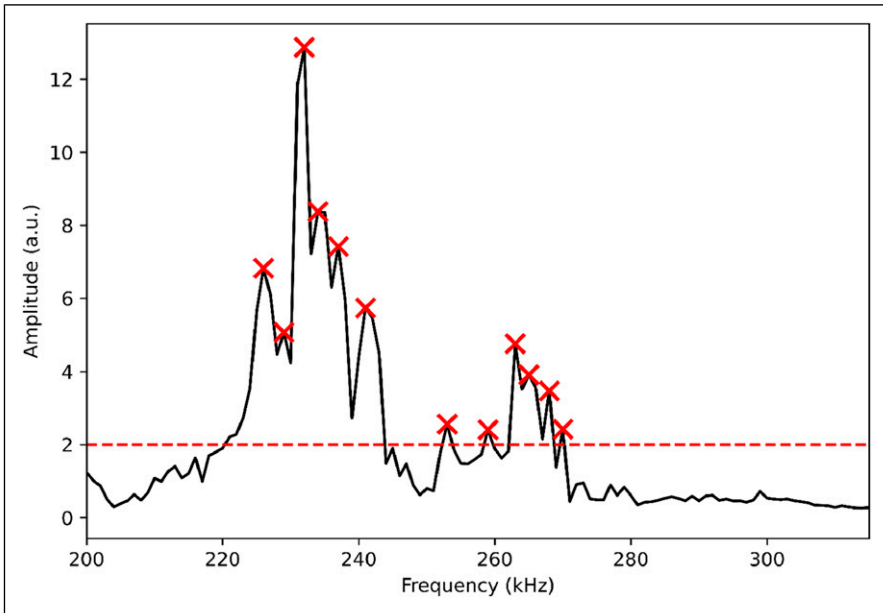


Figure 3. Determined frequency peaks shown with X, identified for an extruded FFT signal. The threshold line can be seen, which limits the script from identifying any peaks below the associated amplitude range. The Y-axis represents the signal amplitude (a.u.), the X-axis represents the frequency (kHz).

on the moduli and density of the material components. Crystalline structures with compact internal structures limit the expansion / contraction caused by the wave, allowing propagation much faster through the medium while amorphous content experience more changes, slowing down the mechanical wave. This is not a linear relation, as various bending modes, either symmetrical or antisymmetrical, exist within the ultrasonic domain. The acoustic dispersion curves were calculated to display the phase velocity at various frequencies within the polymer melt; this velocity is the rate at which waves propagate through materials at various frequencies. Plotting these curves provided an understanding about which dispersion mode(s) were associated with the peaks being monitored in this study. The calculations were done using the open-sourced *Lamb-Wave-Dispersion* Python package (Version 0.0.0).¹⁷ To calculate the dispersion modes, the melt channel thickness, h , longitudinal speed of sound c_L and transverse speed of sound c_S were required. These speeds of sound were calculated using the theoretical elastic modulus E , shear modulus G and density ρ of the melt at a given fiber content:

$$c_L = \sqrt{\frac{E}{\rho}} \quad (1)$$

$$c_S = \sqrt{\frac{G}{\rho}} \quad (2)$$

These two moduli are temperature sensitive, causing changes to the speed of sound. The measured melt temperature values for these calculations were collected according to the method discussed in the composite preparation section, with averaged values given in Table 1. From the table, there appeared to be an increase in the melt temperature as the melt velocity increased, which brought about a corresponding decrease in the moduli and speed of sound values. Above the melting point of a neat polymer the speed of sound will decrease by a constant rate.^{18–20} For polypropylene, this rate has been shown by others to be roughly 0.04% per °C.^{19,20} When a fiber is introduced into the melt, the rate has been seen to increase, with others reporting values ranging from 2 to 10 times that of the neat polymer matrix.²¹ To consider the effect of increasing melt temperature seen in Table 1, the speeds of sound and material moduli were first calculated at the melting point of polypropylene (165°C); each modulus based on fiber content was estimated by the rule of mixtures using data for both polymer and glass found in the literature at this temperature.^{22,23} The rates at which the speeds of sound decreased were chosen to be 5 times the rate of polypropylene, resulting in both c_L and c_S decreasing by 0.2%/°C above the melting temperature. This can be expressed by equation (3):

$$c_i(T) = c_{i, T_m} [1 - 0.2\%(T - T_m)], \text{ where } i = L \text{ or } S, \text{ and } T > T_m \quad (3)$$

Examples of calculated dispersion curves are shown in Figure 4, plotted alongside an acoustic spectrum collected at the die for the exiting composite melt, where both the antisymmetric (A4, A5) and symmetric (S3, S4) modes phase velocities are seen at the respective frequency range.

Statistical methods

Several statistical methods were applied in this work using Python. The first method was to identify statistical differences in the fiber length from each operating state in the extruder. The Kolmogorov-Smirnov (KS) similarity test, using the SciPy 'kstest' function, was conducted on the CDFs and evaluated against each other. Three KS tests were

Table 1. The average melt temperature for the 30 weight percent tapes exiting at various flow velocities.

Flow velocity (mm/min)	Temperature (°C)
80	224
160	246
240	250
320	253

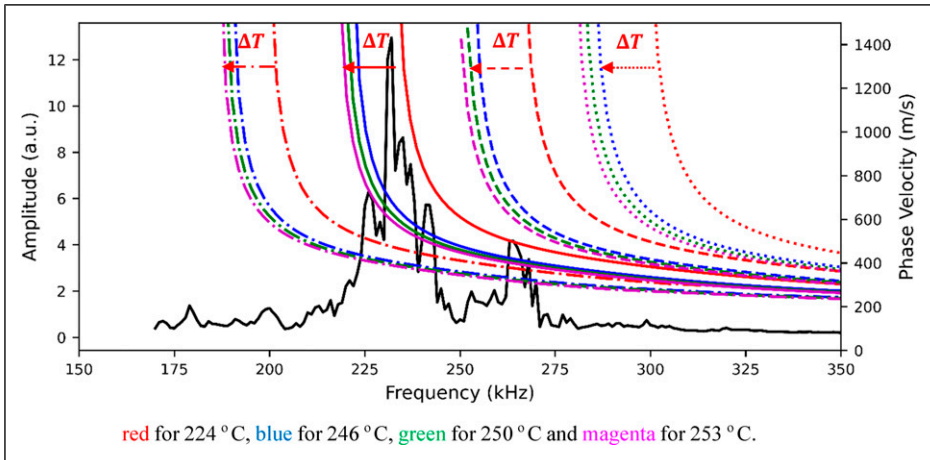


Figure 4. Simulated dispersion mode results for increasing melt temperature caused by changing melt velocity, plotted with an extruded FFT signal. The dashdot lines (— · —) represent the symmetric S3 mode, the solid lines (—) represent the antisymmetric A4 mode, the dashed lines (---) represent the symmetric S4 mode and the dotted (· · ·) lines represent the antisymmetric A5 mode. The colours represent the melt temperature, red for 224 °C, blue for 246 °C, green for 250 °C and magenta for 253 °C. The arrows indicate the transition of the modes as the melt temperature changes, changing the frequencies of the dominant modes.

conducted for each distribution pair; is distribution A different from distribution B ($H_o : A(x) = B(x)$); is distribution A greater than distribution B ($H_o : A(x) \leq B(x)$); is distribution A less than distribution B ($H_o : A(x) \geq B(x)$).

The second method used Principal Component Analysis (PCA) to differentiate frequencies influenced by the fiber content versus melt velocity in the collected spectra. The principal components were calculated using the NumPy library, and the spectral data was mean centered for each frequency band. For each melt velocity, score plots of the first two principal components compared the clustering of results for each extruded fiber content. The score plots, seen in the supplementary figure, Figure S3, displayed the scores for each individual fiber weight fraction clustered separately from one another. The separation of the scores indicated there were clear differences in the spectra for each weight fraction. PCA was also used to determine if the clustering behavior was present for a single plot regardless of melt velocity. The score plot indicated that each fiber weight fraction other than the polypropylene samples were unable to cluster separately, there was a large degree of score overlap occurring. The scores must be separated by melt velocity to clearly demonstrate clustering region.

The third method explored the impact melt velocity had on the peak frequency value. The variability of the peak frequency as the melt velocity changed was calculated using the NumPy library. The variability was calculated for each processing condition and for each peak, and then averaged. The variability was quantified as the standard deviation in peak frequency over the four melt velocities

for each of the 12 peaks, assessed for each of the six fiber weight fractions and polypropylene. The calculated variability provided insight into how much the peaks were shifting by this phenomenon with melt velocity to ensure it was not related to experimental variability.

Finally, an analysis of experimental variability was explored through repeated trials over 3 days. There were sufficient time gaps between the 3 days chosen, with the extruder extensively cleaned after each run. Using the NumPy library, the experimental variability was calculated as the standard deviation in peak frequency over the 3 days of repeated trials. For each specific peak and fiber weight fraction that was repeated, the variability over the melt velocity (physical phenomenon) was compared with the variability over the 3 days of repeated trials (experimental uncertainty). The comparisons could yield three conclusions; larger variability in the physical phenomenon indicated that the shifted peak was a systematic issue rather than due to experimental uncertainty; larger variability in the experimental uncertainty would disregard the peak from further consideration; similar magnitudes of variability result in no conclusions to be drawn.

Results

Process-dependent shifting of the mean peak frequency

The acquired acoustic signals that passed through the molten flow field were compared based on the glass fiber weight fraction present and the melt velocity, to determine the effect of these variables on the frequency of each peak under study. To aid in observing trends among the twelve regions determined in the ultrasound signal analysis section, the mean frequency for each respective range was evaluated for a given extrusion condition; this method of using the mean peak frequency was done in a previous work as to manage the large datasets generated by the acoustic sensors.¹⁴ Figure 5 plots each of the twelve determined mean frequencies as polymer melt velocity increased, based on fiber weight fraction. Since the shift behavior with pure polypropylene was distinctly different from the fiber-filled, its variability was separately stated. The averaged variability in frequency shift was $\pm 0.33\text{kHz}$ for the fiber-filled samples and $\pm 0.50\text{ kHz}$ for the pure polypropylene samples, matching our observations of the data in Figure 5.

With specific consideration for fiber content as an influential variable, the peak frequencies were found to be unaffected; the peaks in spectra occurred at the same determined frequencies regardless of fiber content at each velocity. Melt velocity had the only significant impact on the peak frequencies, which is not a previously noted phenomenon in the literature. The shifts in frequency for the baseline sample (0 wt% fiber fraction) were much larger than with fibers present, as mentioned above, especially for the frequency peaks of 227–229 kHz, 229–232 kHz, 232–235 kHz, 258–261 kHz, 264–266 kHz, and 266–269 kHz. Some of the frequency peaks showed greater variability with changing melt velocity than others, notably at 227–229 kHz and 240–244 kHz with both showing a shift to higher frequencies as the melt velocity increased. Other peaks, such as 235–240 kHz and 252–255 kHz demonstrated very little variability with changing melt

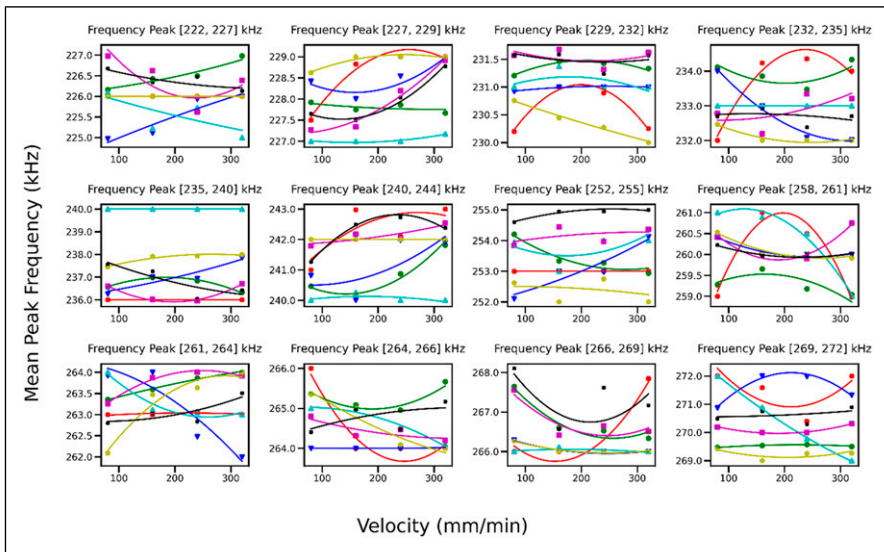


Figure 5. Mean frequency position for each of the 12-significant peak ranges (symbols), fitted with a $y = x^2$ regression curve (solid lines). The 0 wt % data is indicated in red x, the 5 wt % data is indicated in green ●, the 10 wt % data is indicated in blue ▼, the 15 wt % data is indicated in cyan ▲, the 25 wt % data is indicated in magenta ■, the 30 wt % data is indicated in yellow ◆ and the 40 wt % data is indicated in black +.

velocity, where excluding one or two outlier trials, their mean peak frequency remained statistically unchanged in each case.

The possibility of a correlated interaction between fiber weight fraction and melt velocity was considered and not found to be significant. The PCA analysis conducted earlier tested the entire dataset, not just subsets based on melt velocity, and was unable to differentiate the fiber-filled scores as they clustered on top of one another. The inability to differentiate the data without the need to separate based on the melt velocity led to this assertion that there was no interaction to be influencing the frequency shift phenomenon.

The following is an analysis of potential cause, attempting to dismiss all but one explanation for the frequency shifting phenomenon associated with melt processing. Since this phenomenon interferes with accurately correlating acoustic signals with end product properties, the goal was to determine whether, based on cause, the issue could be avoided or simply accommodated.

Discussion

The observed frequency shifting that initiated this study impeded attempts to establish a correlation between material properties and the acoustic signal by an inline monitoring system meant to provide quality assurance for polymer composite manufacturing.

Working within the frequency domain is rather attractive for non-destructive monitoring because multiple descriptors of the product can foreseeably be recorded simultaneously if a unique spectral fingerprint can be correlated to each characteristic. This frequency shifting phenomenon, if not compensated, will invariably produce incorrect values from those correlations should changes in flow rate be a normal part of operations, making understanding of the matter important. To understand the phenomenon, three hypotheses were postulated and then explored below. These hypotheses were that (1) melt temperature changes attributed to viscous dissipation influenced the acoustic dispersion mode of the melt; (2) velocity associated changes in the heterogeneous melt composition passing between the two sensors were causing the shift; or (3) the signal was sensitive to shear damage of the glass fibers, notably their length distribution, with varying flow rates. The analyses will show that a changing dispersion mode was the most likely cause for the phenomenon.

Changing dispersion mode

For sound propagation, both the longitudinal and transverse speeds of sound are proportional to the medium (polymer melt) temperature, decreasing as the system temperature increases (which also results in a corresponding decrease in modulus of the medium).^{18,20,21} Since changing melt temperature would be expected with changing fiber content or polymer melt velocity due to viscous dissipation and an altered shear distribution,²⁴ the dispersive behavior of the acoustic waves within a polymer melt may explain the shifts in mean frequency seen at the die; dispersive materials experience signal attenuation dependent upon frequency and if this nature was changing, peaks in an acoustic spectrum would appear to shift as a result. To explore this nature as the cause for the peak shifting observed, dispersion curves were first calculated for pure polypropylene over the range of recorded melt temperatures (Table 1). The curves can be seen within the supplementary file in Figure S4. At the lower melt temperature conditions (224°C), associated with faster speeds of sound, a single dispersion mode for the studied spectral region can be identified as the antisymmetric A4 mode. As melt velocity and correspondingly melt temperature increased, the effects of viscous dissipation caused a reduction in the moduli of polymer melt, decreasing the speed of sound. This change in speed caused a shift in the frequencies of the acoustic wave which may easily propagate through the polymer melt to lower values in the analyzed spectral region; in other words, the A4 mode had shifted towards lower frequencies. The impact of the altered modal frequencies appeared to be substantial for most of the recorded frequencies but not all. Of the twelve studied frequency peaks, only four did not indicate any non-linear change to the peak frequency as the melt velocity changed, those being the 222–227 kHz, 235–240 kHz, 252–255 kHz and 261–264 kHz peaks. The lack of change is a result of these frequency regions not being influenced by polypropylene but rather by the glass fibers, which we noted are less dispersive materials than the polymer matrix.

To calculate the dispersion curves in Figure 4 for the fiber-filled composite and then simulate the effect of temperature during processing on the melt, a mixed material approach was used, as described in the dispersion mode determination section; the example

of simulated modes shown in the figure corresponded to a glass fiber weight fraction of 30 wt%. This method of calculation captured the combined effects of fiber weight fraction and melt velocity in the dispersion curves. At the lower temperature conditions associated with faster speeds of sound (224°C), the antisymmetric A4 mode was once again identified as the dominant mode for the studied spectral region, with the greatest phase velocity at 234 kHz. Unlike the pure polypropylene modal analysis where only a single mode was present, the symmetric S4 mode was also present at the edge of the spectral region, with the greatest phase velocity being at 267 kHz. The same modal shifts seen in the pure polypropylene analysis were observed for the fiber-filled composite with the frequencies of the modes decreasing as the speed of sound decreased from increasing melt temperature. This shift resulted in two dominant modes. The frequencies of the A4 and S4 modes with the greatest phase velocity would change based on the fiber content, however the behavior of the changing modes would be seen for all extruded materials. Unlike the results with pure polypropylene which had some frequency peaks not experiencing any shift with melt velocity, all twelve peaks displayed notable changes for the fiber-filled results indicating this phenomenon was consistently appearing for all fiber weight fractions. There were some exceptions to this; 10 wt% experienced no shifts for the 264–266 kHz peak; 15 wt% experienced no shifts for either the 232–235 kHz peak nor the 235–240 kHz peak; and 30 wt% experienced no shifts for the 222–227 kHz peak nor the 240–244 kHz peak. The reason why these peaks did not experience this shifting phenomenon can be related back to the modes themselves. These dispersion modes are highly dependent on the speed of sound travelling through the polymer melt and decrease by a fixed rate associated with temperature as discussed in the dispersion mode determination section. Glass is a natural sound insulator and the speed of sound in our glass fibers decreased at a large rate per change in temperature than the polymer, and so acoustic signals propagating became increasingly dampened as glass content increased, making certain peaks appear negligibly affected by this phenomenon.

The greater variation in frequency shifting (based on melt velocity) with pure polypropylene compared to the glass-filled composites can be explained by the number of shifting modes present within the analyzed spectral region; average variation in peak frequency shift was ± 0.33 kHz for the glass-filled composite compared to ± 0.50 kHz for pure polypropylene. The increase in the number of modal descriptors indicates that there will be more frequencies easily propagating through the polymer melt with limited impedance. For the fiber-filled experiments having two modes, one at the lower frequencies and the other at the higher frequencies of the analyzed spectral region, the recorded frequencies will resonate accordingly with those modes. The $\sim 50\%$ increase in variability for the pure polypropylene compared to the fiber-filled can be related to where the identified peak frequencies are relative to the modal frequencies. The modal frequencies calculated in [Figure 4](#) for the composite indicate that the first six identified peaks were best described by the A4 mode and the final six identified peaks were best described by the S4 mode; when both of those modes shift to the lower frequencies due to viscous dissipation the surrounding peak frequencies to those modes will change. The pure polypropylene experiments only had the singular mode present in the entire analyzed frequency region; all twelve identified peaks were described by the A4 mode. There also

is the consideration of the acoustic properties of the glass reducing the degree of variability in the case of the composite. As discussed earlier, the speed of sound for glass decreased at a much larger rate relative to temperature change compared to pure polypropylene and glass is a natural sound insulator, hence signal dampening occurred at the respective peak frequencies for the fiber-filled melt that diminished the system sensitive to melt velocity.

We are acknowledging that this may not fully explain why the shifts are occurring, but it is the best explanation for the changing behavior. The recorded frequencies are highly dependent on the mode, as the frequency of the modes changes the recorded frequencies at each of the individual peaks will change accordingly. There is strong support from this analysis for variation in melt temperature on dispersion modes as the cause for peaks experiencing frequency shifts in our testing. This appears to be a real and novel effect for active acoustic monitoring of continuous processing not previously shown in the literature. However, two other possible effects still need to be considered.

Doppler effects

Doppler effects are more commonly attributed to fast moving objects (e.g., vehicles) but have also been considered in the biomedical field for much slower phenomena such as determining cardiovascular blood flow where velocities more closely match those in our die.^{25–27} Hence, the second hypothesis explored the possibility of a doppler shift affecting our acoustic signal. Normally, signals demonstrating a doppler shift were collected using a pulse-echo protocol with a single sensor. When the emitter and receiver are separate and not in the same location, the differences in sensor positions need to be accounted for, which causes a bistatic doppler moment.²⁸ The equation for a bistatic doppler moment is given as:

$$f_D = 2f \frac{v}{c_s} \cos\left(\frac{\beta}{2}\right) \cos(\delta) \quad (4)$$

where v is the theoretical melt velocity, f_D is the frequency shift, c_s is the speed of sound, and β and δ are geometric constraints related to the sensor locations. To explore the feasibility of a bistatic moment, we sought to determine the velocity of the medium passing through the die to cause a shift in the mean peak frequencies of the detected signal by 1 kHz as this magnitude of shift was very common during the extrusion trials. The calculation used an emitted frequency of 220 kHz, and a speed of sound for pure polypropylene (225°C) of 921 m/s.¹⁹ Based on the layout of the PEEK rods within the extruder die, the geometric factors for the bistatic plane $\frac{\beta}{2}$ and δ become 52 ° and 38 °. Solving equation (4) for \vec{v} , the polymer melt would need to be traveling at just over 222 m/min, for a bistatic doppler moment of 0.86 kHz to be experienced. The maximum velocity of the polymer melt was 320 mm/min, orders of magnitude slower than the speed necessary for a typical 0.86 kHz shift observed in the polymer melt for pure polypropylene. The earlier mentioned cardiovascular studies were tested at a higher frequencies (1 – 10 MHz) and per equation (4) the velocity \vec{v} necessary for a doppler shift would

therefore be smaller.^{29–31} Since the present system was analyzed in the kHz range and not the MHz range, a doppler moment can only be observed at speeds well above what was being used. It was concluded that no doppler moment was experienced in these trials.

Changing fiber length distribution

Another hypothesis that was explored was whether shear-dependent fiber breakage, a known issue in twin-screw compounding operations, was correspondingly affecting the acoustic signal; it has been previously shown that glass fiber breakage increases with its increasing weight fraction in a composite during extrusion but also that breakage decreases with increasing melt flow rate.^{32–35} The screw speed would also have an influence on the fiber length, decreasing the length until a critical fiber length is achieved.^{34,36} Since the screw speed was maintained at 100 RPM, determining if this critical value was achieved was not explored, and the effects of screw speed were negated. Since the resonance frequency of a glass fiber is inversely proportional to the square of its fiber length, any statistically significant change to the fiber length distribution should change the overall resonance frequency of the glass phase in the melt and possibly impact the detected signal.¹⁴

The fiber length distribution for the trial condition of 10 wt% and 80 mm/min for fiber content and melt velocity, respectively appeared to have longer fibers than those for the 40 wt% and 320 mm/min condition. To test for significance, the KS test described in the statistical methods section was performed on the CDFs. Each of the eight CDFs were compared against one another using three KS tests (different, greater than, less than) to determine if any underlying distributions were statistically different, resulting in 28×3 KS tests being conducted. For each of the 84 KS tests, the null hypothesis was only rejected for two repeats at the 40 wt% and 320 mm/min condition for fiber content and melt velocity, respectively. All other distributions spanning the tested range of experiments showed no statistical difference. This may indicate the critical fiber length was achieved, and that the shear forces exerted onto the fibers within the extrusion system were too small to cause further fiber damage.^{34,36} Based on the near negligible changes in fiber length found, this hypothesis for explaining the frequency shifting was dismissed.

Repeatability

To confirm the observed frequency shifts changing with melt velocity were repeatable physical phenomenon and distinctive from experimental uncertainty, an expanded set of trials was conducted. The compounding of 5 wt%, 25 wt% and 40 wt% fiber loaded blends was repeatedly done over several days in a random order, with two additional melt velocities added at 120 and 200 mm/min included in the testing. The plots for the respective frequency ranges were provided as Supplementary information in [Figure S5](#) where the same shifting phenomenon is seen in comparison to the original trials (the results section). The KS tests for significance found once again that there were no underlying differences in the fiber length distributions, even for the new melt velocity conditions.

A full visual comparison between the two variability sets can be seen in the Supplementary Information in [Figure S6](#). In general, larger variability associated with the physical phenomenon was found for all twelve analyzed peaks recorded during the new trials with the 25 wt% and 40 wt% glass-filled composites. For the 5 wt% glass-filled composite, shifting seen by most peaks in the results section was attributed to the physical phenomenon, however, experimental uncertainty could not be dismissed as an explanation for shifts corresponding to the 264–266 kHz peak; both measures of variability were similar (± 0.69 kHz).

In this analysis, the peaks showing high repeatability in the magnitude of shifting over the tested range of melt velocities (and being distinctive from experimental uncertainty) corresponded to those at 229–232 kHz and 261–264 kHz, varying by ± 0.50 kHz and ± 0.51 kHz respectively; these would be considered robust peaks for identifying the shifting phenomenon. These specific frequency regions are quite close to the theoretical A4 mode (234 kHz) and S4 mode (267 kHz), with the slight differences being likely attributed to how speeds of sound were estimated in the dispersion mode determination section for elevated temperatures; the rate at which the speed of sound decreased with temperature may have been larger in the experiments than what was calculated. Furthermore, the peaks that experienced the highest magnitude in shifting across the melt velocities (and being distinctive from experimental uncertainty) were identified as the peaks at 232–235 kHz and 266–269 kHz, with variabilities of ± 1.09 kHz and ± 1.08 kHz respectively with the repeated set of trials. Interestingly, these peaks were at frequencies just slightly higher than the highly repeatable peaks mentioned above. This suggests the frequencies slightly higher than the modal frequencies will experience the largest degree of shift within the composite melt.

Conclusions

Glass fiber reinforced polypropylene composites at different weight fractions was compounded in a twin screw extruder at varying velocities and monitored with active acoustics to develop a quality assurance system for the industry. In the course of the system development, it was observed that the recorded signals changed as flow rate changed, presenting a challenge in correlating frequencies in the monitored signal to material properties. The observed frequency shifts were noticeable in twelve distinct frequency regions. Through analysis of the changing signal under different processing conditions, the shifting phenomenon was attributed to local modulus changes in the polymer melt causing the dominant acoustic dispersive modes to shift towards lower frequencies, influencing the analyzed spectra. These local moduli changes were related to viscous dissipation as the melt velocity increased. This effect was stronger for pure polypropylene compared to the fiber-filled composite due to the glass fibers which dampened the phenomenon. The repeatability in this shifting over multiple trials demonstrated the physical phenomenon was not an artifact of experimental uncertainty.

Acknowledgements

They would also like to thank Paul Gatt and Thomas Wire Die (Burlington, Canada) for aid in developing the extrusion die and PEEK buffer rods; Hassan Abdulhussain, Jierui Jian, Vladimir Gritsichine and Heera Marway for aid during extrusion trials; the International Composite Research Group (ICRG), Dr. Natalia Nikolova and Andy Krbavac for conceptual aid during the studies; and Doug Culley for ashing the extruded tape samples.

Declaration of conflicting interests

The author(s) declared no potential conflicts of interest with respect to the research, authorship, and/or publication of this article.

Funding

The author(s) disclosed receipt of the following financial support for the research, authorship, and/or publication of this article: The authors would like to thank both the NSERC Collaborative Research and Training Experience (CREATE) Program: Advanced Polymer Composite Materials and Technologies No. 401209347 and the Deutsche Forschungsgemeinschaft (DFG, German Research Foundation), project number 255730231, within the International Research Training Group “Integrated engineering of continuous-discontinuous long fiber-reinforced polymer structures” (GRK 2078) for the joint funding of this project.

ORCID iD

Austin D Bedrosian  <https://orcid.org/0000-0003-2086-6058>

Supplemental Material

Supplemental material for this article is available online.

References

1. Böhlke T, Hrymak A, Kärger L, et al. 1 - introduction to continuous-discontinuous fiber-reinforced polymer composites. In: Böhlke T, Henning F, Hrymak A, et al. (eds). *Continuous-Discontinuous Fiber-Reinforced Polymers*. Munich: Hanser, 2019, pp. 1–10.
2. Krautkrämer J and Krautkrämer H. *Ultrasonic testing of materials*. Berlin, Heidelberg: Springer Berlin Heidelberg, 1990.
3. Anugonda P, Wiehn JS and Turner JA. Diffusion of ultrasound in concrete. *Ultrasonics* 2001; 39(6): 429–435.
4. Saad AK, Abdulhussain HA, Gomes FPC, et al. Studying the mechanism of biodiesel acting as an environmental stress cracking agent with polyethylenes. *Polymer* 2020; 191: 122278.
5. Fey P, Meiler S, Kreutzbruck M, et al. Non-contact inline monitoring of thermoplastic CFRP tape quality using air-coupled ultrasound. *AIP Conf Proc*. 2019; 2055(1): 120001.
6. James V, Carswell D, Riise J, et al. Robot deployed Laser-Ultrasonic NDT system for inspection of large aircraft structures. *IOP Conf Ser Mater Sci Eng* 2021; 1024: 012032.
7. Lizaranzu M, Lario A, Chiminelli A, et al. Non-destructive testing of composite materials by means of active thermography-based tools. *Infrared Phys Technol* 2015; 71: 113–120.

8. Tan KT, Watanabe N and Iwahori Y. X-ray radiography and micro-computed tomography examination of damage characteristics in stitched composites subjected to impact loading. *Compos B Eng* 2011; 42(4): 874–884.
9. Bakic PR, Li C, West E, et al., (eds) *Comparison of 3D and 2D breast density estimation from synthetic ultrasound tomography images and digital mammograms of anthropomorphic software breast phantoms*. Bellingham: Proc SPIE, 2011.
10. França DR, Jen CK, Nguyen KT, et al. Ultrasonic in-line monitoring of polymer extrusion. *Polym Eng Sci* 2000; 40(1): 82–94.
11. Gholizadeh A, Mansouri H, Nikbakht A, et al. Applying acoustic emission technique for detecting various damages occurred in PCL nanomodified composite laminates. *Polymers* 2021; 13(21): 3680.
12. McClements DJ and Fairley P. Ultrasonic pulse echo reflectometer. *Ultrasonics* 1991; 29(1): 58–62.
13. James RM. *Acoustic emission*. New York: Gordon and Breach Science Publishers Inc., 1983.
14. Bedrosian AD, Thompson MR, Hrymak A, et al. Developing a supervised machine-learning model capable of distinguishing fiber orientation of polymer composite samples nondestructively tested using active ultrasonics. *J Adv Manuf Process*. 2022; 5(1).
15. Faber J, Vistein M, Chaloupka A, et al., (eds) *Sensor-based process monitoring of in-situ polymerization in T-RTM manufacturing with caprolactam*. SAMPE Europe Conference, 2021.
16. Tsuda H, Lee J-R, Guan Y, et al. Investigation of fatigue crack in stainless steel using a mobile fiber Bragg grating ultrasonic sensor. *Opt Fiber Technol* 2007; 13(3): 209–214.
17. Rotea F. Lamb-wave-dispersion. *GitHub* 2023, [cited 2023 April 12]. <https://github.com/franciscorotea/Lamb-Wave-Dispersion>
18. Lionetto F and Maffezzoli A. Polymer characterization by ultrasonic wave propagation. *Adv Polym Technol* 2009; 27(2): 63–73.
19. Nayfeh TH, Abu-Zahra NH, Fedek WM, et al. Ultrasound measurement of two-Filler concentrations in polypropylene compounds. Part 1: static calibration. *Int J Adv Des Manuf Technol* 2002; 20(4): 313–318.
20. Praher B, Straka K, Usanovic J, et al. Ultrasound based monitoring of the injection moulding process - methods, applications and limitations. *AIP Conf Proc* 2014; 1593: 159–162.
21. Nomura R, Yoneyama K, Ogasawara F, et al. Temperature dependence of sound velocity in high-strength fiber-reinforced plastics. *Jpn J Appl Phys* 2003; 42(8): 5205–5207.
22. Li J, Zhu Z, Li T, et al. Quantification of the young's modulus for polypropylene: influence of initial crystallinity and service temperature. *J Appl Polym Sci*. 2020; 137(16): 48581.
23. Shibukawa T, Gupta VD, Turner R, et al. Temperature dependence of shear modulus, density, and crystallinity of isotactic poly polypropylene. *Textil Res J* 1962; 32(12): 1008–1010.
24. Coates PD, Barnes SE, Sibley MG, et al. In-process vibrational spectroscopy and ultrasound measurements in polymer melt extrusion. *Polymer* 2003; 44(19): 5937–5949.
25. McIntosh DH, Rix HW, Rieke MJ, et al. Redshifted and blueshifted broad lines in luminous quasars. *Astrophys J* 1999; 517(2): L73–L76.
26. Nishimura RA, Miller FA, Callahan MJ, et al. Doppler echocardiography: theory, instrumentation, technique, and application. *Mayo Clin Proc* 1985; 60(5): 321–343.

27. Pham V-H, Taieb MH, Chouinard J-Y, et al. On the double Doppler effect generated by scatterer motion. *REV Journal on Electronics and Communications*. 2011; 1(1).
28. Chen VC. *The micro-Doppler effect in radar*. London: Artech House, 2019.
29. Hoskins PR. Simulation and validation of arterial ultrasound imaging and blood flow. *Ultrasound Med Biol* 2008; 34(5): 693–717.
30. Koratala A and Reisinger N. Venous excess Doppler ultrasound for the nephrologist: pearls and pitfalls. *Kidney Med* 2022; 4(7): 100482.
31. Mohamed AA, Arifi AA and Omran A. The basics of echocardiography. *J Saudi Heart Assoc* 2010; 22(2): 71–76.
32. Thomason JL, Owens E and Fiberglas C. The influence of fibre length and concentration on the properties of glass fibre reinforced polypropylene: 5. Injection moulded long and short fibre PP. *Composites Part A* 2002; 33: 1641–1652.
33. Ville J, Inceoglu F, Ghamri N, et al. Influence of extrusion conditions on fiber breakage along the screw profile during twin screw compounding of glass fiber-reinforced PA. *Int Polym Process* 2013; 28(1): 49–57.
34. Le Baillif M and Oksman K. The effect of processing on fiber dispersion, fiber length, and thermal degradation of bleached sulfite cellulose fiber polypropylene composites. *J Thermoplast Compos Mater* 2009; 22(2): 115–133.
35. Tungjitpornkull S, Chaochanchaikul K and Sombatsompop N. Mechanical characterization of E-chopped strand glass fiber reinforced wood/PVC composites. *J Thermoplast Compos Mater* 2007; 20(6): 535–550.
36. Huang M, Zu Y, Wang H, et al. Critical length prediction for fiber breaking in injection molded of long-fiber reinforced thin-walled products. *J Thermoplast Compos Mater*. 2024; 08927057241296469.